Available online at www.sciencedirect.com
ScienceDirect
Trans. Nonferrous Met. Soc. China 33(2023) 1029−1037
Transactions of Nonferrous Metals Society of China
www.tnmsc.cn

Interface structure and properties of spray-forming (SiC_p+β-$LiAlSiO_4$)/6092Al matrix composites

Cai-he FAN[1,2], Wen-jing HE[1], Ze-yi HU[1], Qin WU[1], Yu-meng NI[1]

1. College of Materials and Advanced Manufacturing, Hunan University of Technology, Zhuzhou 412007, China;
2. Anhui Jianye Science and Technology Co., Ltd., Huaibei 235000, China

Received 29 November 2021; accepted 24 May 2022

Abstract: 45 wt.% SiC_p/6092Al, 5 wt.% β-$LiAlSiO_4$/6092Al and (45 wt.% SiC_p + 5 wt.% β-$LiAlSiO_4$ (Euc))/6092Al matrix composites were successfully fabricated by spray-forming and die forging technology. The microstructures, interface structures, and phase composition of the composites were analyzed with optical microscope (OM), scanning electron microscope (SEM), transmission electron microscope (TEM), and X-ray diffractometer (XRD). The thermal expansion properties, bending strength, and bending modulus of the composites were tested by thermal dilatometer and electro-mechanical universal testing machines, respectively. The results show that the SiC_p and β-$LiAlSiO_4$ (Euc) particles are uniformly distributed in the 6092Al matrix, and a strong bonding interface is formed with the Al matrix. The SiC_p/Al, and Euc/Al interfaces of the (45 wt.% SiC_p+5 wt.% Euc)/6092Al matrix composite are straight and clear. However, the interface reaction is not found. After solution treatment and artificial aging (T6), the coefficient of thermal expansion (CTE), bending strength, and bending modulus for (45 wt.% SiC_p + 5 wt.% Euc)/6092Al matrix composites are 14.68×10^{-6} K^{-1} in the temperature range of 303−473 K, 589 MPa, and 165 GPa, respectively.

Key words: spray-forming; Al matrix composites; interface structure; coefficient of thermal expansion (CTE); bending strength; bending modulus

1 Introduction

Due to the requirement of working environment, high strength and low expansion coefficient is becoming more and more important for the reliability and life spans of satellite structural parts. At present, it is urgent to develop particle reinforced Al matrix composites with high strength, low expansion and high thermal conductivity to replace Ti alloy, which can reduce the weight of satellite structural parts and reduce the production cost [1,2].

Many preparation methods have been proposed to fabricate SiC_p/Al composites with high volume fraction of SiC, such as stirring casting, powder metallurgy, and pressure impregnation [3,4]. However, these methods have several disadvantages. For example, the particles are not evenly dispersed, easy to agglomerate and have interface reaction to generate brittle phase, which greatly reduces the comprehensive properties of composites [5]. In recent years, spray-forming technology has been adopted to SiC_p/Al composites with high volume of SiC_p, which has many advantages, such as uniform particle dispersion, fast cooling rate, fine grain size, uniform microstructure and low oxidation degree, and can reduce the formation of Al_4C_3 at the interface effectively [6].

SiC_p has the characteristics of high strength, excellent wear resistance, and low thermal expansion, etc., and has been widely used in the fields of high-temperature structural materials, friction materials, thermal insulation materials, and

Corresponding author: Cai-he FAN, Tel: +86-731-22183432, E-mail: 369581813@qq.com
DOI: 10.1016/S1003-6326(23)66163-1

building materials [7,8]. The density of SiC_p (3.216 g/cm^3) is lower than that of TiC (4.93 g/cm^3), TiB_2 (4.52 g/cm^3), and Al_2O_3 (3.5 g/cm^3), and the price for SiC_p is also the lowest. It can be used to reduce the weight of satellites and the cost of satellite production and launch. In recent years, scholars have conducted much research on spray-forming SiC_p/Al matrix composites. WU et al [9] have prepared 15 vol.% SiC_p/7075Al composites with uniform distribution and small porosity of SiC_p by spray-forming. The composites show super-plasticity at a deformation temperature of 723 K and strain rate of 0.001−0.1 s^{-1}. YUAN et al [10] have prepared ultra-high-strength SiC_p/Al composite by spray-forming and extrusion process, with an elastic modulus of 100 GPa and a tensile strength of 785 MPa. β-$LiAlSO_4$ (Euc) particles are important types of negative expansion material, and the coefficients of thermal expansion (CTEs) along *a*-axis and *c*-axis of the cell are 7.8×10^{-6} and -17.5×10^{-6} K^{-1}, respectively [11]. XUE et al [12] have prepared Euc/Cu composites by the vacuum hot pressing sintering method with a relatively low CTE. It has been found that the increases in the volume fraction of Euc particles simultaneously decrease the CTE and thermal conductivity of the composites. WANG et al [13] have found that the CTE of Euc/Cu composites decreased with the reduction of residual stress by annealing, and the lowest CTE is obtained after thermal cycling at 323−632 K. In conclusion, the existing research is mainly focused on SiC_p or Euc particle single-phase reinforced metal matrix composites, while the research on SiC_p and Euc particles hybrid reinforced 6092Al matrix composites is rarely reported.

In this work, SiC_p and Euc particles hybrid reinforced 6092Al matrix composites were prepared by spray-forming and die forging technology. The effects of SiC_p and Euc particles on the micro-structure, interface structure, and properties of the composites were studied, which laid a theoretical foundation for the industrial application of SiC_p and Euc particles hybrid reinforced Al matrix composites.

2 Experimental

The 6092Al alloy was used as the matrix material, and the positive expansion material, SiC_p, and the negative expansion material, Euc particles, were used as the reinforcement phase. The chemical composition of 6092Al is given in Table 1. The physical properties of the matrix and reinforcing particles are given in Table 2. The schematic of the experimental setup is shown in Fig. 1.

Table 1 Chemical composition of 6092Al alloy (wt.%)

Mg	Cu	Si	Fe
0.80−1.20	0.70−1.00	0.40−0.80	0.30

Zn	Ti	O	Others	Al
0.25	0.15	0.05−0.50	0.15	Bal.

Table 2 Physical properties of matrix and reinforcing particles

Raw material	Size/ μm	Density/ (g·cm^{-3})	CTE/ 10^{-6} K^{-1}
6092Al	−	2.70	23.20
SiC_p	2−6	3.21	6.58
Euc particles	2−8	2.60	−6.20

The 45 wt.% SiC_p/6092Al, 5 wt.% Euc/6092Al, and (45 wt.% SiC_p + 5 wt.% Euc)/6092Al matrix composites were prepared on SF380 large-scale injection molding equipment, which were named as Sample 1, Sample 2, and Sample 3, respectively. The Al alloy was smelted in a graphite crucible with a melting temperature of 1053 K, and the entire smelting and refining process was protected by anhydrous N_2 to avoid oxidation. Gas blowing treatment [14,15] is an effective way to refine 6092Al alloys. After refining the Al alloy, the temperature was raised to 1103 K, and the molten metal was poured into the preheated graphite crucible through a sealed flow channel. The molten metal in the crucible flowed out through a liquid guiding tube with an inner diameter of 3−5 mm and was fogged in the atomizer. SiC_p and Euc particles were also transported to the atomizer by a quantitative powder feeding device, and the particles were fully mixed with high-pressure N_2 (pressure of 1.2−1.6 MPa) in the atomizer to form a solid−gas two-phase flow. SiC_p, Euc particles, atomized solid, and liquid particles were deposited on a circular iron substrate plate 100−250 mm away from the atomizer to prepare SiC_p and Euc particles hybrid reinforced Al matrix composites deposited billet with the size of *d*150 mm × 1000 mm. The composite billets were firstly processed into a round

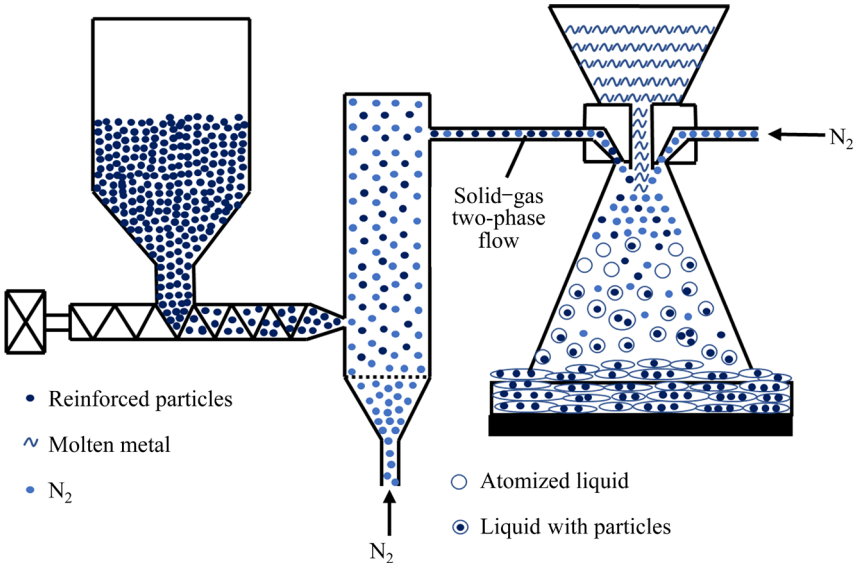

Fig. 1 Schematic of experimental setup

ingot of *d*120 mm × 200 mm and placed in a forging mold, then heated to 863 K for 1 h, and finally pressed on a 315 t press for 20 s. The master cylinder pressure and stroke of 315 t press are 3.15×10^6 N and 300 mm, respectively. After demolding, the sample was turned over 180°, and forged again with the same process. Finally, Sample 1, Sample 2, and Sample 3 were subjected to solution treatment and artificial aging of solid solution treatment at 793 K for 1.5 h and artificial aging at 443 K for 3 h.

The morphology and distribution of reinforced particles in the Al matrix were observed by DMC4500 (OM) and Quanta 650 FEG (SEM). The microstructure and interface structure of the samples were analyzed by JEOL 2100 (TEM) and the connected energy spectrometer was used to analyze the elemental composition of the samples. The transmission samples were mechanically pre-thinned to approximately 70 μm and then ion thinned. The thermal expansion performance was tested on an L75VS1600 thermal dilatometer with the sample size of *d*6 mm × 30 mm, and the heating rate of 3 °C/min.

3 Results

3.1 Microstructure

The metallographic image of Sample 3 is illustrated in Fig. 2. As illustrated, SiC_p and Euc particles are uniformly distributed in the Al matrix without agglomeration. The typical SEM micro-

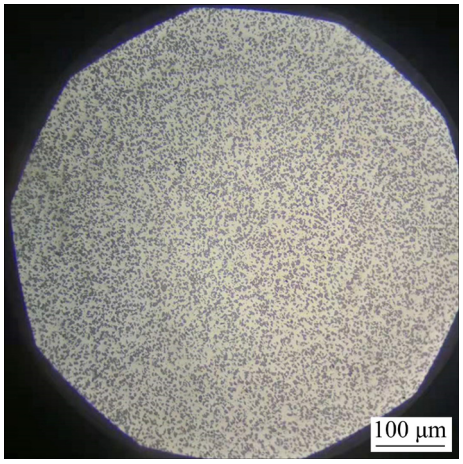

Fig. 2 Morphological distribution of SiC_p and Euc particles in 6092Al matrix

structures of Sample 1, Sample 2, and Sample 3 are shown in Fig. 3. As can be seen from Figs. 3(a, b), there are two regions in the secondary electron (SE) image, namely the Al matrix and SiC_p. As shown in Fig. 3(c), there are three regions in the SE image, which are the Al matrix, SiC_p, and Euc particles, respectively. The line scan energy spectrograms (EDS) of Figs. 3(d) and 3(e) correspond to Line 1 and Line 2 in Fig. 3(c), respectively. According to the change in Al and Si element contents in Fig. 3(d), it can be judged that this particle is SiC_p. According to the change of Al, Si, and O element contents in Fig. 3(e), it can be judged that this particle is a Euc particle. As shown in Figs. 3(a−c), a large number of irregular SiC_p and a small amount of Euc particles are uniformly dispersed in the Al matrix.

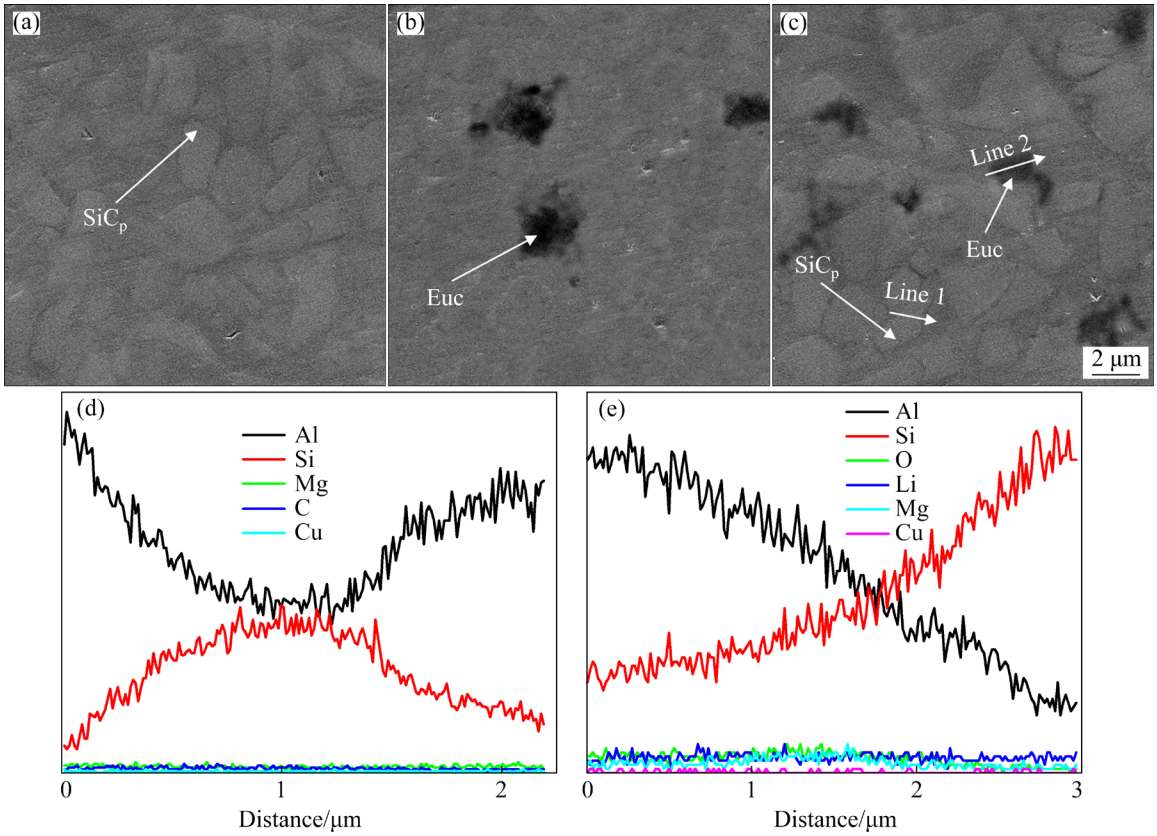

Fig. 3 SEM images of Sample 1 (a), Sample 2 (b), and Sample 3 (c), and scan energy spectra for Line 1 (d) and Line 2 (e) in Fig. 3(c)

3.2 Interface structure

Figure 4 shows TEM images of the interface between the reinforcing particles and the Al matrix of Sample 3 after T6 treatment. As shown at the SiC_p/Al interface of Sample 3 (Fig. 4(a)), the SiC_p in the composites is a typical hexagonal close-packed 6H-SiC with a 6-layer period, which belongs to α-SiC. According to the diffraction spots in the figure, the black regular area is SiC_p (2), and the gray area is α(Al) (1). The SiC_p/Al interface is clear and smooth, and no reactants are generated. As shown at the Euc/Al interface of Sample 3 (Fig. 4(b)), the Euc/Al interface is clear and no interfacial reaction occurs. According to the diffraction spots, the black region is Euc particles (4), while the gray region is α(Al) (3). The images in the upper right corner of Figs. 4(a, b) are high-resolution TEM images of the SiC_p/Al interface and Euc/Al interface. The atoms near the SiC_p/Al interface and Euc/Al interface are closely arranged, and the interface is clean, flat, straight, and no other reactants are formed. The interplanar spacings of SiC_p and Euc particles are d=0.251 nm and d=0.215 nm, respectively.

The X-ray diffraction patterns of Sample 1, Sample 2, and Sample 3 after T6 treatment are shown in Fig. 5. It can be seen that the main phase compositions of Sample 1 are α(Al) and 6H-SiC, those of Sample 2 are α(Al) and Euc, with a few Mg_2SiO_4 and $LiAlSi_2O_6$ phases, while those of Sample 3 are α(Al), 6H-SiC and Euc.

3.3 Property

3.3.1 Thermal expansion properties

The thermal expansion curves of the (SiC_p + Euc)/6092Al composites with different mass fractions at 303−473 K are shown in Fig. 6. It is shown that the CTE of the Al matrix composites increases with the increase of temperature. At temperatures below 373 K, the CTE increases rapidly; however, the increase tends to be gentle with temperatures higher than 373 K. The mass fraction of SiC_p and Euc particles has a significant effect on the linear expansion properties of the composites. With the increase of the mass fraction of Euc particles, the linear expansion coefficient of the composites decreases significantly. Table 3 shows that the CTEs of Sample 1, Sample 2, and

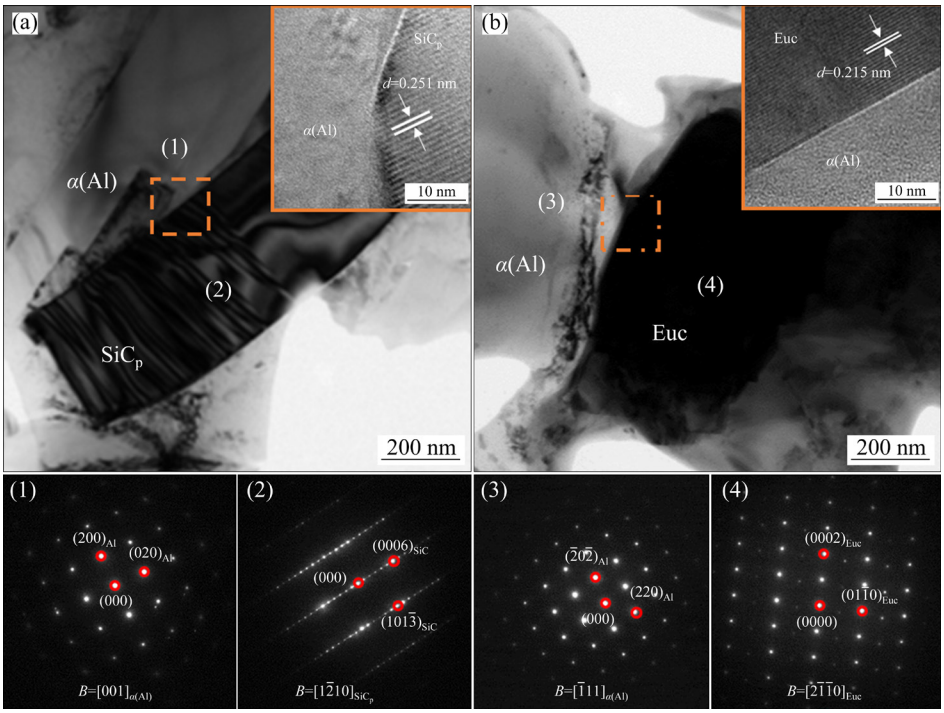

Fig. 4 TEM images of reinforcing particle/matrix interface and diffraction spots of reinforcing particles in Sample 3: (a) SiC_p/Al interface; (b) Euc/Al interface

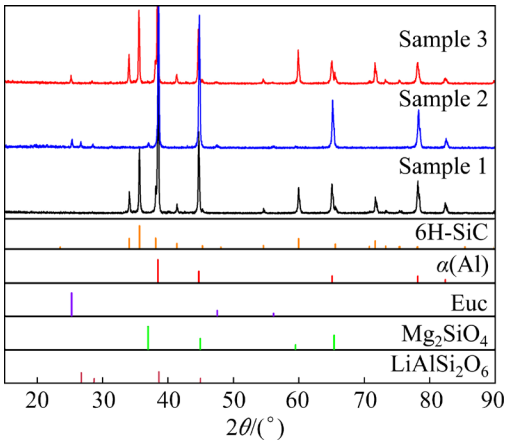

Fig. 5 XRD patterns of composite samples after T6 treatment

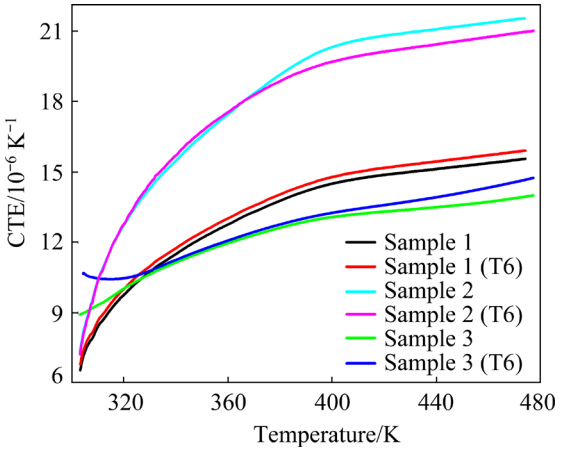

Fig. 6 CTE of (SiC_p + Euc)/6092Al composites in temperature range of 303−473 K

Sample 3 in the temperature range of 303−473 K are 15.58×10^{-6}, 21.54×10^{-6}, and 14.07×10^{-6} K^{-1}, respectively. Figure 6 also shows the comparison of CTE curves of the composites before and after T6 treatment. As shown, the CTEs of Sample 1, Sample 2, and Sample 3 after T6 treatment show little change compared with those before T6 treatment. As can be seen from Table 3, the CTEs of Sample 1, Sample 2, and Sample 3 in the temperature range of 303−473 K after T6 treatment are 15.89×10^{-6}, 21.51×10^{-6}, and 14.68×10^{-6} K^{-1}, respectively.

3.3.2 Mechanical properties

As shown in Table 3, after T6 treatment, the bending strength values of Sample 1, Sample 2, and Sample 3 are 613, 355, and 589 MPa, respectively, and the bending moduli are 172, 82, and 165 GPa, respectively. The densities of Sample 1, Sample 2, and Sample 3 are 2.85, 2.60 and 2.75 g/cm^3, respectively, measured by the Archimedes principle. Solid solution treatment at 793 K for 1.5 h and artificial aging at 443 K for 3 h increase the density, bending strength and modulus of the composites.

Table 3 CTE, density, bending strength, and bending modulus of composite samples

Sample No.	At forging state				After T6 treatment			
	CTE/ 10^{-6} K^{-1}	Density, ρ/(g·cm^{-3})	Bending strength, σ/MPa	Bending modulus, E/GPa	CTE/ 10^{-6} K^{-1}	Density, ρ/(g·cm^{-3})	Bending strength, σ/MPa	Bending modulus, E/GPa
1	15.58	2.85	494	113	15.89	2.92	613	172
2	21.54	2.60	302	46	21.51	2.67	355	82
3	14.07	2.75	485	96	14.68	2.82	589	165

For Sample 3 after the heat treatment, the higher solid solution temperature makes the Al matrix have a certain fluidity. The Al matrix gradually fills the pores during the solid solution process, which promotes the densification. The heat treatment makes the Al matrix and the reinforcing particles more closely combined, and the interface area between the particles and the matrix increases. When the composite is under load, the soft matrix can more effectively transfer the load to the hard SiC_p through the interface, thereby improving the bending strength of the composites. This is consistent with the findings of HONG et al [16], whose study showed that the thermo-mechanical properties of the SiC_p/Al composites are mainly attributed to the changes in the degree of densification and interfacial bonding. Incomplete densification and poor interface bonding may cause poor interface conductance and weak bending strength.

4 Analysis and discussion

4.1 Interface analysis

The interface of composite material refers to the small area between the matrix and the reinforcement particles where the chemical composition changes significantly and the composites combine for load transfer. As can be seen from Fig. 4(a), SiC_p/Al and Euc/Al interfaces of Sample 3 are flat, clean, and continuous without precipitates, and hole defects. It can be inferred that the interface structure of Sample 3 is a direct atomic bonding between the reinforcing particles and the matrix. According to the diffraction spots in Fig. 4, the SiC_p has hexagonal crystals with a lattice constant a=0.308 nm, and the α(Al) phase is composed of face-centered cubic crystals with a lattice constant a=0.405 nm. The phase interface is formed between two adjacent phases with different crystal structures and grain orientations. The calculation of the lattice misfit for the SiC_p and α(Al) phases is 23%; that is to say, the SiC_p/Al interface is approximately a semicoherent interface, which indicates that the SiC_p/Al interface in Sample 3 has a strong bonding.

SiC_p/Al interface exists in several types, such as obviously reactive interface, slightly reactive interface, and clean interface [17]. The obviously reactive interface refers to the continuous reaction layer generated by the reaction between SiC_p and Al matrix. The interface reactants are usually brittle phases, Al_4C_3 or $MgAl_2O_4$. The continuous interface reaction layer composed of these brittle phases is prone to crack initiation under tensile load, which is seriously detrimental to the performance of composites [18]. The slightly reactive interface refers to the interface with discrete distribution of reactants at the SiC_p/Al interface and the step interface. From the viewpoint of wettability, as long as a small amount of discontinuous small reactants appear on the interface of the composite material, the wettability between SiC_p and Al will be improved, thereby realizing the effective transfer of load from matrix to reinforcement [19,20]. The clean interface is formed by atomic bonding between SiC_p and Al. Through the TEM image analysis (Fig. 4), the clean interfaces obtained in this experiment are all chemically bonded clean interfaces formed by tight atomic matching. And the X-ray diffraction pattern (Fig. 5) shows that the main phase compositions in the composite material sample are α(Al), 6H-SiC and Euc. It can be inferred that no interfacial reaction occurs when the Al matrix composites are prepared by spray-forming technology and die forging technology.

Figure 7 shows the TEM image of Sample 3. As can be seen, dislocations are observed near the SiC_p/Al interface and in the Al matrix. This probably results from the large difference in CTE among SiC_p, Euc particles, and Al matrix. In the cooling process after forging, the thermal residual

stress is generated between the matrix and the reinforcement due to their synchronous shrinkage. To release the accumulated thermal residual stress, dislocations are generated in the matrix, leading to the work hardening of the composite. During the preparation process, the matrix undergoes plastic deformation to increase the dislocation density, resulting in the strengthening of the matrix, thereby improving the mechanical properties of the composites.

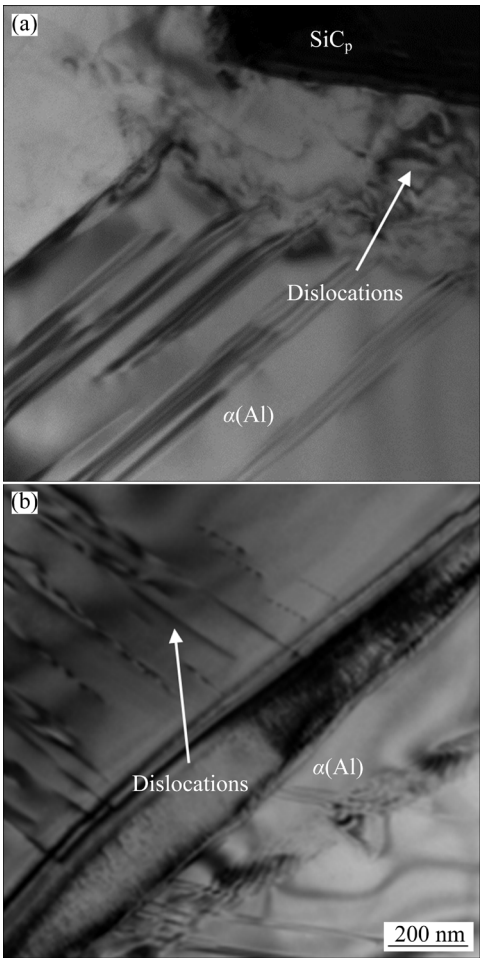

Fig. 7 TEM images of Sample 3: (a) Dislocation near SiC_p/Al interface; (b) Dislocation within α(Al)

4.2 Properties of composite materials

The CTE is used to characterize the change in the volume or length of materials when heated, and it is one of the important thermophysical properties of Al matrix composites. The CTE can be divided into linear expansion coefficient and volume expansion coefficient. In this work, the effects of the mass fraction and T6 treatment on the linear expansion coefficient of Al matrix composites were studied.

The reinforcing particles of Sample 3 are uniformly distributed in the matrix, the atoms near the SiC_p/Al and Euc/Al interfaces are closely arranged, and the interface is clean and straight. In the process of thermal expansion, the reinforcing particles can constrain the expansion effect of the matrix, thus reducing the CTE of the material. Euc particles have strong atomic bonding bonds. When the temperature rises, the expansion of atomic spacing is not obvious, the crystal lattice changes dynamically, and the flexible structure occupies the original blank part in the crystal lattice, so Euc particles present negative expansion. In the temperature range of 303−473 K, the average coefficient of linear expansion of Sample 3 is the lowest, $14.07\times10^{-6}\,K^{-1}$, which is 9.69% and 34.68% lower than that of Sample 1 and Sample 2, respectively.

As shown in Fig. 6, all the linear expansion coefficients of the composites decrease in the presence of SiC_p and Euc particles in the Al matrix. This is consistent with previous works, because the CTE of SiC_p and Euc particles is much lower than that of the Al matrix [21,22]. In addition, the CTE of composite samples can also decrease as the mass fraction of SiC_p and Euc particles increases. The CTE of the Al matrix composites reinforced by particles with different mass fractions has little change after T6 treatment, because the thermal expansion properties of the composites are mainly related to the properties and mass fraction of reinforced particles [23,24].

It can be seen from Table 3, the bending strength and modulus of Sample 1 are the largest, followed by Sample 3, and those of Sample 2 are the least. When the content is low, the reinforcing particles can disperse in the Al matrix and improve the deformation resistance of the Al matrix by hindering dislocation movement or the coordinated deformation of grain boundaries [25]. The higher the particle content is, the smaller the average particle spacing is, and the more significant the enhancement effect is. When the volume content of reinforcing particles is equal to that of Al matrix, especially when the ceramic particles generate a three-dimensional interconnected skeleton network in the Al matrix, the coordination deformation ability of the Al alloy grain is seriously restricted by the rigid ceramic particles, and the plasticity of

the composite is reduced, but the brittleness is significant [26]. Excessive reinforcing particles content makes the composites brittle, resulting in the decrease of strength. This phenomenon is consistent with the effect of SiC_p volume fraction on the bending strength and modulus of materials studied by LIU et al [27]. When SiC_p volume fraction varies from 39% to 62%, the bending strength of SiCp/Al composites increases first and then decreases, and reaches the maximum value when the SiC_p volume fraction is 52%. When the content of reinforcing particles is low, the Al matrix has some plastic deformation ability, and the strength of the composites increases with the increase of content. When the content is too high, the brittleness of composites increases, and the strength decreases.

5 Conclusions

(1) The (45 wt.% SiC_p + 5 wt.% Euc)/6092Al matrix composites prepared by spray-forming and die forging have been successfully applied to the preparation of the structures of satellite. The SiC_p and Euc particles are uniformly distributed in the 6092Al matrix. The SiC_p/Al and Euc/Al interfaces of the (45 wt.% SiC_p + 5 wt.% Euc)/6092Al matrix composites are straight and clear with no hole defects, and interface reaction are not found.

(2) After solution treatment and artificial aging, the value of CTE for the (45 wt.% SiC_p + 5 wt.% Euc)/6092Al matrix composites is 14.68×10^{-6} K^{-1}, which is the lowest in the temperature range of 303−473 K. The bending strength and modulus of the (45 wt.% SiC_p + 5 wt.% Euc)/6092Al matrix composites after solution treatment and artificial aging are 589 MPa and 165 GPa, respectively, which are increased by 65.92% and 101.2% compared with 5 wt.% Euc/6092Al without SiC_p.

(3) The (45 wt.% SiC_p + 5 wt.% Euc)/6092Al matrix composites have good comprehensive mechanical properties due to their excellent bonding interface, high dislocation density, and dispersed strengthening particles.

Acknowledgments

This work was financially supported by the Major Special Projects in Anhui Province, China (No. 202003c08020005), the Key Projects in Hunan Province, China (No. 2020GK2045), the Science and Technology Innovation Program of Hunan Province, China (No. 2021RC4036), and Postgraduate Scientific Research Innovation Project of Hunan Province, China (No. CX20211079).

References

[1] JASWINDER S, AMIT C. Overview of wear performance of aluminium matrix composites reinforced with ceramic materials under the influence of controllable variables [J]. Ceramics International, 2016, 42(1): 56−81.

[2] FAN Cai-he, YAN Hong-ge, PENG Ying-biao, ZHOU Wei, ZHOU Xing-ling. Microstructures and mechanical properties of spray-forming high magnesium aluminum alloy during large strain hot rolling [J]. The Chinese Journal of Nonferrous Metal, 2017, 27(1): 64−71. (in Chinese)

[3] WOO D J, HEER F C, BREWER L N, HOOPER J P, OSSWALD S. Synthesis of nanodiamond-reinforced aluminum metal matrix composites using cold-spray deposition [J]. Carbon, 2015, 86: 15−25.

[4] GAO Wen-li, SU Hai, ZHANG Hui, LIU Hong-bo, WANG Jian-hua. Microstructure and mechanical properties of spray co-deposited SiC_p/2024 composites [J]. The Chinese Journal of Nonferrous Metals, 2010, 20(1): 49−54. (in Chinese)

[5] WANG Han, ZHANG Hai-ming, CUI Zhen-shan, CHEN Zhe, CHEN Dong. Compressive response and micro-structural evolution of in-situ TiB_2 particle-reinforced 7075 aluminum matrix composite [J]. Transactions of Nonferrous Metals Society of China, 2021, 31(5): 1235−1248.

[6] SHARMA V, PRAKASH U, KUMAR B M. Microstructural and mechanical characteristics of AA2014/SiC surface composite fabricated by friction stir processing [J]. Materials Today Proceedings, 2015, 2: 2666−2670.

[7] AHMADI A, TOROGHINEJAD M R, NAJAFIZADEH A. Evaluation of microstructure and mechanical properties of Al/Al_2O_3/SiC hybrid composite fabricated by accumulative roll bonding process [J]. Materials Design, 2014, 53: 13−19.

[8] ZHU Shi-ze, MA Guo-nan, WANG Dong, XIAO Bo-lv, MA Zong-yi. Suppressed negative influence of natural aging in SiC_p/6092Al composites [J]. Materials Science and Engineering A, 2019, 767: 1−10.

[9] WU Hong-dan, ZHANG Hui, CHEN Shuang, FU Ding-fa. Flow stress behavior and processing map of extruded 7075Al/SiC particle reinforced composite prepared by spray deposition during hot compression [J]. Transactions of Nonferrous Metals Society of China, 2015, 25(3): 692−698.

[10] YUAN Wu-hua, ZHANG Jian, ZHANG Chen-chen, CHEN Zhen-hua. Processing of ultra-high strength SiC_p/Al−Zn−Mg−Cu composites [J]. Journal of Materials Processing Technology, 2009, 209(7): 3251−3255.

[11] WANG Li-dong, XUE Zong-wei, CUI Y, WANG K P, QIAO Y J, FEI Wei-dong. Thermal mismatch induced disorder of beta-eucryptite and its effect on thermal expansion of beta-eucryptite/Al composite [J]. Composites Science and Technology, 2012, 72: 1613−1617.

[12] XUE Zong-wei, LIU Zhe, WANG Li-dong, FEI Wei-dong. Thermal properties of new copper matrix composite reinforced by β-eucryptite particulates [J]. Metal Science

Journal, 2013, 26(12): 1521−1524.
[13] WANG Li-dong, XUE Zong-wei, LIU Zhe, FEI Wei-dong. Thermal expansion behavior of a β-$LiAlSiO_4$/Cu composite [J]. Rare Metals, 2009, 28(1): 82−85.
[14] LI Feng, XING Peng-fei, LI Da-gang, ZHUANG Yan-xin, TU Gan-feng. Removal of phosphorus from metallurgical grade silicon by Ar−H_2O gas mixtures [J]. Transactions of Nonferrous Metals Society of China, 2013, 23(11): 3470−3475.
[15] WU Ji-jun, MA Wen-hui, LI Yan-long, YANG Bin, LIU Da-chun, DAI Yong-nian. Thermodynamic behavior and morphology of impurities in metallurgical grade silicon in process of O_2 blowing [J]. Transactions of Nonferrous Metals Society of China, 2013, 23(1): 260−265.
[16] HONG Yu, WANG Wu-jie, LIU Jia-qin, TANG Wen-ming, WU Yu-cheng. Effect of porosity and interface structures on thermal and mechanical properties of SiC_p/6061Al composites with high volume fraction of SiC [J]. Transactions of Nonferrous Metals Society of China, 2019, 29(5): 941−949.
[17] KONG Ya-ru, GUO Qiang, ZHANG Di. Review on interfacial properties of particle-reinforced aluminum matrix composites [J]. Materials Reports, 2015, 29(5): 34−43.
[18] CHANG Hao, SUN Jian, CHEN Guo-hong, WANG Bing, YANG Lei, ZHANG Jian-hua, TANG Wen-ming. Microstructure and properties of high-fraction graphite nanoflakes/6061Al matrix composites fabricated via spark plasma sintering [J]. Transactions of Nonferrous Metals Society of China, 2021, 31(6): 1550−1560.
[19] ZHAO Wen-min, BAO Rui, YI Jian-hong, HOU Xiang-hui, FANG Dong, LIU Chun-xuan. Fabrication of RGO/Cu composites based on electrostatic adsorption [J]. Transactions of Nonferrous Metals Society of China, 2020, 30(4): 982−991.
[20] MA Guo-nan, WANG Dong, LIU Zhen-yu, XIAO Bo-lv, MA Zong-yi. An investigation on particle weakening in T6-treated SiC/Al–Zn–Mg–Cu composites [J]. Materials Characterization, 2019, 158: 1−32.
[21] ZAN Yu-ning, ZHOU Yang-tao, LIU Zhen-yu, WANG Quan-zhao,WANG Wen-guang, WANG Dong, XIAO Bo-lv, MA Zong-yi. Microstructure and mechanical properties of (B_4C+Al_2O_3)/Al composites designed for neutron absorbing materials with both structural and functional usages [J]. Materials Science and Engineering A, 2020, 773: 1−9.
[22] ZHANG Shu-gang, CHEN Liang, LI Zhi-gang, ZHAO Guo-quan, ZHANG Cun-sheng. Investigation on microstructure and mechanical properties of in-situ TiB_2/Al−Cu−Mg composite profile fabricated by porthole die extrusion [J]. Materials Science and Engineering A, 2020, 786: 139449.
[23] CHAO Z L, SUN T T, JIANG L T, ZHOU Z S, CHEN G Q, WU G H. Ballistic behavior and microstructure evolution of B_4C/AA2024 composites [J]. Ceramics International, 2019, 45(16): 1−6.
[24] FAN Cai-he, OU Ling, HU Zei-yi, YANG Jian-jun, CHEN Gang, YAN Hong-ge. Microstructures and mechanical properties of BP/7A04 Al matrix composites [J]. Transactions of Nonferrous Metals Society of China, 2019, 29(10): 2027−2034.
[25] IMANIAN GHAZANLOU S, EGHBALI B, PETROV R. EBSD characterization of Al7075/graphene nanoplates/carbon nanotubes composites processed through post-deformation annealing [J]. Transactions of Nonferrous Metals Society of China, 2021, 31(8): 2250−2263.
[26] BI Jiang, LEI Zheng-long, CHEN Xi, LI Peng, LU Nan-nan, CHEN Yan-bin. Microstructure and mechanical properties of TiB_2-reinforced 7075 aluminum matrix composites fabricated by laser melting deposition [J]. Ceramics International, 2019, 45(5): 5680−5692.
[27] LIU Jun-wu, ZHENG Zhi-xiang, WANG Jian-min, WU Yu-cheng, TANG Wen-ming, LÜ Ju. Pressureless infiltration of liquid aluminum alloy into SiC preforms to form near-net-shape SiC/Al composites [J]. Journal of Alloys and Compounds, 2008, 465(1/2): 239−243.

喷射成形(SiC_p+β-$LiAlSiO_4$)/6092Al 基复合材料的界面结构及性能

范才河[1,2]，何文静[1]，胡泽艺[1]，吴 琴[1]，倪雨朦[1]

1. 湖南工业大学 材料与先进制造学院，株洲 412007；2. 安徽建业科技有限公司，淮北 235000

摘 要：采用喷射成形技术和模锻工艺成功制备 45% SiC_p/6092Al、5% β-$LiAlSiO_4$/6092Al 和(45% SiC_p+5% β-$LiAlSiO_4$(Euc))/6092Al(质量分数)基复合材料。利用光学显微镜(OM)、扫描电镜(SEM)、透射电镜(TEM)和 X 射线衍射仪(XRD)对复合材料试样的显微组织、界面结构及物相成分进行分析，采用热膨胀仪和电子万能试验机分别对复合材料试样的热膨胀性能、弯曲强度和模量进行测试。结果表明：(45% SiC_p+5% Euc)/6092Al 基复合材料中碳化硅颗粒和 Euc 颗粒在 6092Al 基体中分布均匀，并与铝基体形成强力结合界面，SiC_p/Al 和 Euc/Al 界面平直清晰，没有发现界面反应。复合材料试样经固溶人工时效后，在 303~473 K 温度范围内，(45% SiC_p + 5% Euc)/6092Al 基复合材料试样的线膨胀系数为 14.68×10^{-6} K^{-1}，弯曲强度和模量分别达到 589 MPa 和 165 GPa。

关键词：喷射成形；铝基复合材料；界面结构；热膨胀系数(CTE)；弯曲强度；弯曲模量

(Edited by Bing YANG)